Progress In Electromagnetics Research M, Vol. 54, 91–102, 2017

Calculation of Passive Magnetic Force in a Radial Magnetic Bearing Using General Division Approach

Tapan Santra*, Debabrata Roy, and Amalendu B. Choudhury

Abstract—This paper represents the force calculation in a radial passive magnetic bearing using Monte Carlo technique with general division approach (s-MC). The expression of magnetic force is obtained using magnetic surface charge density method which incurs a multidimensional integration with complicated integrand. This integration is solved using Monte Carlo technique with 1-division (1-MC) and 2-division (2-MC) approaches with a MATLAB programming. Analysis using established methods such as finite element method (FEM), semi-analytical method, and adaptive Monte Carlo (AMC) method has been carried out to support the proposed technique. Laboratory experiment has been conducted to validate the proposed method. 2-MC gives better result than 1-MC. The computation time of the proposed method is compared with the quadrature method, FEM and AMC. It is observed that the proposed method invites less computational burden than those methods as the algorithm adaptively traverses the domain for promising parts of the domain only, and all the elementary regions are not considered with equal importance.

1. INTRODUCTION

A radial magnetic bearing consists of two passive ring magnets [1] in concentric fashion. This bearing is very popular due to its simple construction, contact free operation, zero lubrication, no wear, high rotational speed and zero maintenance [2]. To model the bearing for control, optimization and performance analysis, calculation of force between these two ring magnets is indispensable [3]. So design of such bearing needs to crack the equations of force which is a very complex function of many geometrical and operational parameters. The methods available to solve the equation of force between two ring magnets are finite element method (FEM) [4], three dimensional (3D) numerical method [5], semi-analytical method [6, 7] and analytical method [8, 9]. Lijesh and Hirani [10] developed some analytical equations for design optimization of magnetic bearing.

Among these methods, the 3D numerical technique is preferred due to its high accuracy. The complicated multidimensional integration associated with the 3D numerical method may be solved by different techniques, namely: the quadrature method, Monte Carlo method (MC), Adaptive Monte Carlo method (AMC) etc. The traditional quadrature method is monotonous and laborious too. The crude MC method has high integration error and computational burden. Santra et al. [11] carried out an adaptive Monte Carlo technique (AMC) to calculate the magnetic force, where the wastage in calculation is avoided using importance sampling. The sample density was optimally selected using Lagrangian method in the integration domain [12] in each iteration. Due to this optimization the calculation becomes little bit complicated and difficult to understand.

In this paper, a simple methodology is considered using Monte Carlo technique with general division approach (s-MC) where the sample density remains constant in all the iterations. There are some large peaks in the integration domain which mainly contributes to the integral whereas the flat portions are

Received 6 December 2016, Accepted 19 January 2017, Scheduled 12 February 2017
* Corresponding author: Tapan Santra (tapan_santra98@yahoo.co.in).
The authors are with the Electrical Engineering Department, Indian Institute of Engineering Science & Technology, Shibpur, Howrah, WB, India.

less significant for integration. So, flat distribution of sample points invites error in the calculation unless numbers of samples are very large. On the contrary, if the number of samples is very large computational cost will be high. In this proposed method, the region with maximum estimated error is divided iteratively, and an approximation of the integral is calculated. Finally, addition of the estimated integral of all sub-regions gives the resultant force. In most of the cases the expression of magnetic force contains implicit or elliptic function which really complicates the analysis, but the proposed technique does not depend on the type of the integrand.

In this paper, 1-division (1-MC) and 2-division (2-MC) approaches are considered. It is observed that if the number of divisions s increases the estimated error decreases, but computational time increases. It is observed that the accuracy of this method is more than the semi analytical method [6] and is in close agreement with FEM and experimental results. The computational time also less than other established method such as quadrature method, FEM, and AMC.

2. EXPRESSION OF MAGNETIC FORCE

Figure 1 represents the configuration of a radial passive bearing in the vertical shaft machine. The inner ring magnet is movable and called rotor magnet. The outer magnet is attached to the frame and called stator magnet. Our objective is to find the magnetic force between these two ring magnets due to any kinds of axial and radial movement of the rotor magnets. Fig. 2 shows the translation of rotor magnets along axial and radial direction from their nominal position. Fig. 3 shows the flux distribution pattern between stator and rotor magnet in the bearing. The stator and rotor magnets are axially magnetized along Z-axis, so they have parallel magnetization. We know that bodies with parallel magnetization which repel themselves. When stator and rotor magnet are concentric (Fig. 3(a)), there are symmetric flux distribution in the air gap, so resultant force is zero. When rotor moves axially upwards (Fig. 3(b)) flux density increases at the bottom of the rotor magnet. The rotor magnet experiences an upwards axial force F_a, makes $\frac{dF_a}{dz}$ positive, so this force is destabilizing in nature. When the rotor magnet translates left in radial direction (Fig. 3(c)), flux density increases at the left side air gap, pushing the rotor towards the right, makes $\frac{dF_r}{dx}$ negative, so this force is stabilizing in nature. The nature of the force is also investigated in Section 4. So the radial passive bearing is inherently stable along radial directions but axially unstable.

Figure 4(a) shows the actual magnetic configuration, consisting of two concentric ring magnets with axial polarization. R_1, R_2 are the inner and outer radius of rotor magnet. R_3, R_4 are the inner and outer radius of stator magnet. L_1, L_2 are the thickness of the stator and rotor magnets respectively. To derive

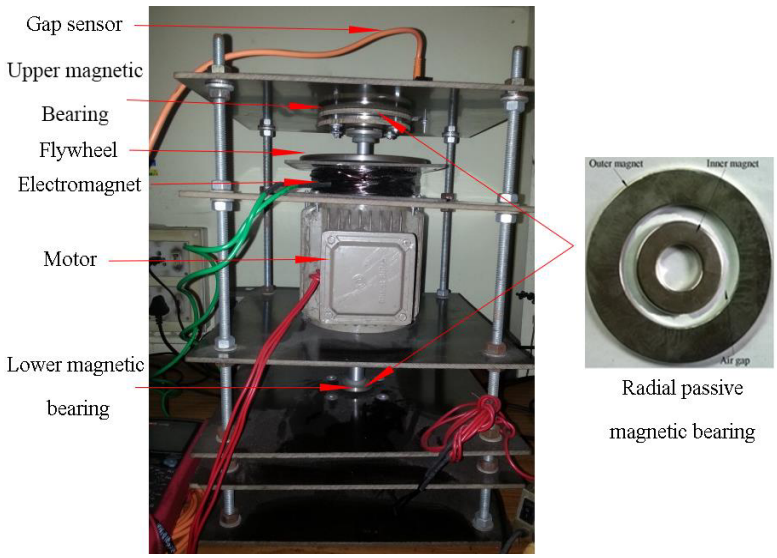

Figure 1. Fabricated model of a vertical shaft machine with radial magnetic bearing.

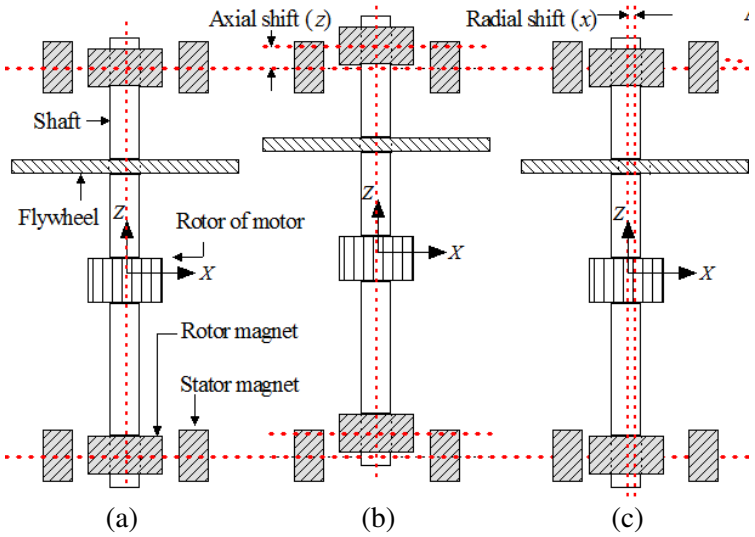

Figure 2. Different motions of rotor. (a) Nominal position. (b) Axial shift along Z axis. (c) Radial shift along X axis.

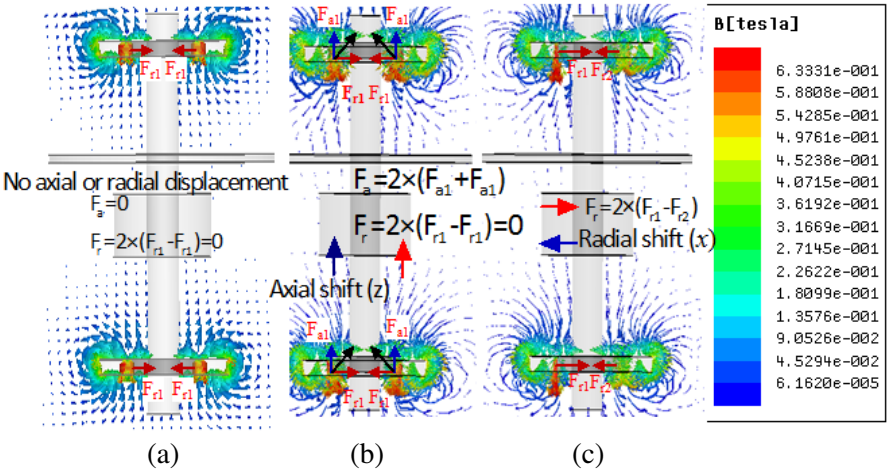

Figure 3. Flux distribution for (a) nominal position of rotor, (b) axial shift of rotor, (c) radial shift of rotor.

the expression of force between two passive magnets, Coulombian surface charge density method [13] is applied. It is assumed that the magnets are uniformly magnetized in the axial z direction as shown in Fig. 4(b). The uniform magnetization (M) has no divergence, so magnetic charge density is zero throughout the volume. Therefore the source of magnetic field (H) is on the top and bottom surfaces of the ring magnets where M originates and terminates. Fig. 4(b) represents the fictive magnetic charge distribution on the top and bottom surfaces of the magnets. In this paper 3D numerical method is applied to calculate the force between stator and rotor magnet due to its high accuracy. Let rotor magnet displaced from nominal position O to O' (Fig. 5(a)) due to a radial shift y along Y-axis and axial offset z along Z-axis. The force between stator and rotor magnet is calculated by Columbian surface charge density method [5] according which it is considered that magnetic charges are distributed on the pole faces A, B, C, and D and they are discretized into small elementary surfaces (Fig. 5(b)). Let $A1$, $B1$, $C1$, and $D1$ are one of such charged magnetic elements. The elementary magnetic force is produced due to the interaction between charges of these elements [14]. There are magnetic forces of attraction ($\vec{F}_{B1C1}$ and $\vec{F}_{D1A1}$) and repulsion ($\vec{F}_{A1B1}$ and $\vec{F}_{C1D1}$) between these charged surfaces. So the total force

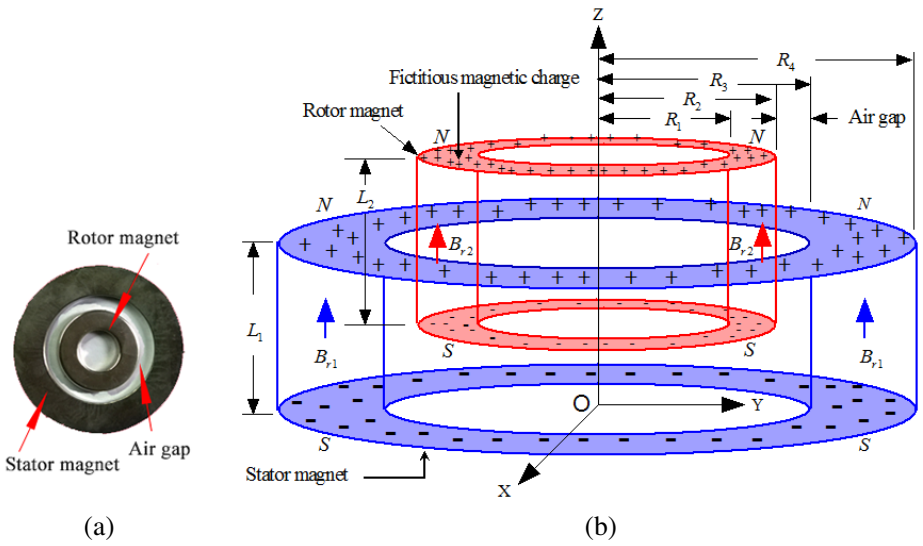

Figure 4. (a) Actual configuration of the radial passive bearing. (b) Magnets with dimensions and charged magnetic faces.

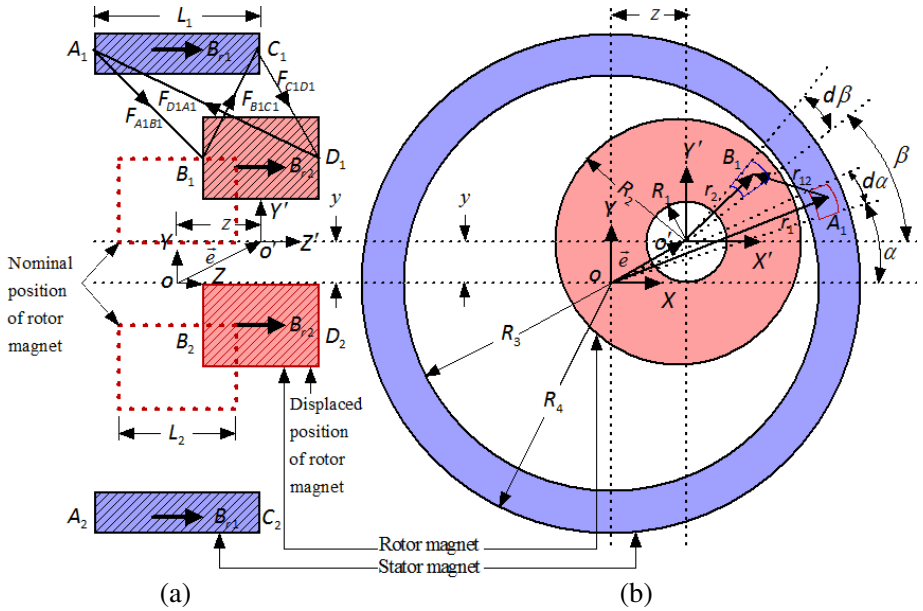

Figure 5. Forces acting on inner magnet after a translation e in Y-Z plane. (b) Elementary force between two tiny magnetic surfaces on outer and inner magnets in Z-X plane.

on rotor is given by the summation of these four forces. By surveying literatures [4, 8, 9], the radial force (F_r) and axial force (F_a) are given by Eqs. (1) and (2) respectively.

$$F_r = \frac{B_{r1}B_{r2}}{4\pi\mu_0}\int_{R_3}^{R_4}\int_{R_1}^{R_2}\int_{0}^{2\pi}\int_{0}^{2\pi}\left[\frac{1}{R_{B1C1}}+\frac{1}{R_{D1A1}}-\frac{1}{R_{C1D1}}-\frac{1}{R_{A1B1}}\right](r_2\sin\beta - r_1\sin\alpha + y)\,dr_1dr_2d\beta d\alpha \quad (1)$$

$$F_a = \frac{B_{r1}B_{r2}}{4\pi\mu_0}\int_{R_3}^{R_4}\int_{R_1}^{R_2}\int_{0}^{2\pi}\int_{0}^{2\pi}\left[\begin{array}{l}\dfrac{z-L_1/2-L_2/2}{R_{B1C1}}+\dfrac{z+L_1/2+L_2/2}{R_{D1A1}}-\dfrac{-z+L_1/2-L_2/2}{R_{C1D1}}\\ -\dfrac{-z-L_1/2+L_2/2}{R_{A1B1}}\end{array}\right]dr_1dr_2d\beta d\alpha \quad (2)$$

Table 1. Parameters of the magnetic system.

Material of magnets	NdFeB
Coercivity (H_{ci})	$1.3 * 10^6$ A/m
Magnetic remanences (B_r)	1.17 T
Outer radius of stator magnet (R_4)	0.025 m
Inner radius of stator magnet (R_3)	0.015 m
Outer radius of rotor magnet (R_2)	0.010 m
Inner radius of rotor magnet (R_1)	0.005 m
Thickness of magnets (T)	0.005 m

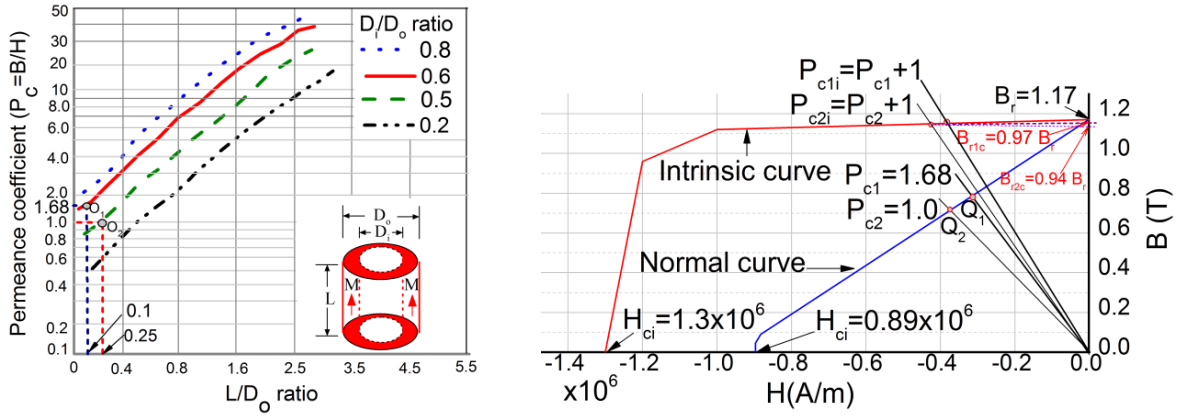

Figure 6. (a) Permeance coefficient (P_c) of axially polarized ring magnet for different dimensions. (b) Calculation of corrected magnetic induction (B_r) considering self demagnetization.

where, B_{r1} and B_{r2} are the corrected magnetic remanences of stator and rotor magnet, respectively. All other symbols and nomenclatures in the equations are self-explanatory and given in Fig. 5.

There is always a continuous process of demagnetization inside a permanent magnet to reduce its energetic state. The geometry of the magnet significantly influences the demagnetizing process. First, the permeance coefficient P_c is calculated as per the literature [15] for ring magnet with axial polarization at open circuit condition as shown in Fig. 6(a). For the given geometry of stator and rotor magnets, listed in Table 1, calculated P_c of stator magnet is $P_{c1} = 1.68$, and rotor magnet is $P_{c2} = 1.0$ as shown in Fig. 6(a). With these P_c values, the corrected magnetic induction is calculated as shown in Fig. 6(b). It is observed that due to demagnetization the stator and rotor magnet induction reduces to $B_{r1c} = 0.97B_{r1}$ and $B_{r2c} = 0.94B_{r2}$ respectively. These modified of magnetic induction will be used for the force calculation using s-MC algorithm.

$$R_{A1B1} = \left((r_2\cos\beta - r_1\cos\alpha)^2 + (r_2\sin\beta - r_1\sin\alpha + y)^2 + (-L_1/2 + L_2/2 - z)^2\right)^{1.5} \quad (3)$$

$$R_{C1D1} = \left((r_2\cos\beta - r_1\cos\alpha)^2 + (r_2\sin\beta - r_1\sin\alpha + y)^2 + (L_1/2 - L_2/2 - z)^2\right)^{1.5} \quad (4)$$

$$R_{D1A1} = \left((r_2\cos\beta - r_1\cos\alpha)^2 + (r_2\sin\beta - r_1\sin\alpha + y)^2 + (L_1/2 + L_2/2 + z)^2\right)^{1.5} \quad (5)$$

$$R_{B1C1} = \left((r_2\cos\beta - r_1\cos\alpha)^2 + (r_2\sin\beta - r_1\sin\alpha + y)^2 + (-L_1/2 - L_2/2 + z)^2\right)^{1.5} \quad (6)$$

Expressions (1) and (2) are the function of four variables r_1, r_2, α and β. The four dimensional visualization of the integrand is very difficult. To visualize the function a coordinate transformation is performed by $\Delta r = r_1 - r_2$ and $\Delta\theta = \alpha - \beta$.

The integrand is plotted in Δr-$\Delta\theta$ plane for inner magnet displacement $y = 0$ and $z = 0.004$ m and

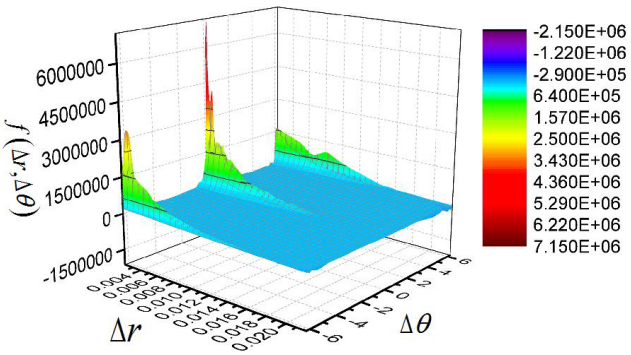

Figure 7. Plot of integrand in two dimensional integration domains.

shown in Fig. 7. It is observed that the main contribution arises from the three peaks in the integration domain, and all other portions are flat and have a minor contribution towards the integration. In this paper, a numerical solution based on Monte Carlo integration technique with general division approach (s-MC) is used to solve Eqs. (1) and (2).

3. MONTE CARLO INTEGRATION WITH GENERAL DIVISION APPROACH (s-MC)

Standard available numerical integration techniques do not perform satisfactorily in multidimensional boundaries, particularly when the integrand is complicated and not smooth. Monte Carlo integration technique [16] is very powerful in these circumstances, mostly for the problem involving integration, which is too difficult to solve analytically and by other available numerical methods. Efficiency of Monte Carlo integration method increases relative to other method when the dimension of the integral increases. Convergence of Monte Carlo method is guaranteed irrespective of problem dimension and smoothness of the function. Monte Carlo is very simple, involves only two steps, random sampling integrand and point evaluation. Consider the problem as shown in Eq. (7).

$$I(f) = \int_{\Omega} f(x)dx \tag{7}$$

where $x \in \Re^d$, $d \geq 1$, $f(x)$ is the function of vector x, and Ω is the d-dimensional hyper rectangle $(a_1, b_1) \times (a_2, b_2) \ldots\ldots (a_d, b_d)$. In crude Monte Carlo (CMC), the integration is done by independently sampling N points $\{x_i\}_{i=1}^{N}$ as per uniform density over Ω and the sample mean is given by Eq. (8).

$$\hat{I}_N = (V/N) \sum_{i=1}^{N} f(x_i) \tag{8}$$

where V is the volume of Ω. If N is very large, then the sample mean $\hat{I}_N$ converges to integration $I(f)$, almost surely. In most of the practical problems, the integrand $f(x)$ varies significantly only in a small portion of overall integration domain Ω. The basic MC, which samples from a uniform distribution U, wastes calculation in the unimportant region. So a systematic procedure is required to allocate resources to the important region of the integration domain. In the proposed method adaptive Monte Carlo technique is used with the general division approach. In most of the integration algorithms an approximation of integration is given by Eq. (9).

$$\tilde{I}_N = \sum_{i=1}^{N} w_i f(x_i) \tag{9}$$

where $x_i \in \Omega$, $i = 1, 2, 3, \ldots, N$ are abscissas or node of integration, and w_i, $i = 1, 2, 3, \ldots, N$ are the weights. The values of weights are corresponding with the appropriate choice of abscissas, with

$\sum_{i=1}^{N} w_i = V$. In this way, the weight of CMC is $w_i = V/N$ for $i = 1, 2, 3, \ldots, N$. In non-adaptive algorithm a fixed set of nodes and weights are used, and it is generated before the evaluation of integration. On the other hand, adaptive algorithm calculates the nodes and weights in present iteration from the result of previous iteration. In our proposed method *global subdivision strategy* [17] is introduced, where the region with largest estimated error is subdivided until the convergence conditions are met.

3.1. Algorithm

Step 1 Set maximum number of iterations M, find the dimension of the problem d, number of random points N in sub-regions and the number of division s, where $0 < s \leq d$.

Step 2 At iteration it, region collection H_{it} contains $it * (2^s - 1) + 1$ number of regions and it is given by Eq. (10)

$$H_{it} = \{\Omega_{it}(j)\}, \tag{10}$$

where $j = 1, 2, 3, \ldots, (it * (2^s - 1) + 1)$.
The creation of sub-regions is explained in Table 1 and Table 2 respectively. Estimate basic Monte Carlo (MC) integration $\hat{I}_{it,j}$ over each regions $\Omega_{it}(j)$. Find out total estimated integral in iteration it over the whole region as per Eq. (11).

$$\hat{I}_{it} = \sum_{j=1}^{(it*(2^s-1)+1)} \hat{I}_{it,j} \tag{11}$$

Step 3 Estimate standard error of integration over the regions $\Omega_{it}(j)$ at iteration it by Equation (12)

$$\hat{E}_{it,j} = V_{it,j} \frac{\hat{\sigma}_f \left|\Omega_{it}(j)\right.}{\sqrt{N_{it,j}}} \tag{12}$$

where $V_{it,j}$ is the volume of region $\Omega_{it}(j)$, $N_{it,j}$ the number of random points taken in $\Omega_{it}(j)$ and $\hat{\sigma}_f \left|\Omega_{it}(j)\right.$ the estimated standard deviation of f over the region $\Omega_{it}(j)$. Total estimated standard error at iteration it over whole region is given by Eq. (13)

$$\hat{E}_{it} = \sqrt{\sum_{j=1}^{(it*(2^s-1)+1)} \hat{E}_{it,j}^2} \tag{13}$$

Step 4 Find out the promising region whose estimated error, $\hat{E}_{it,j}$ is maximum. The index of the promising region is given by Eq. (14)

$$\alpha_{it} = \arg\max \hat{E}_{it,j}, \text{ for } j = 1, 2, 3, \ldots \ (it * (2^s - 1) + 1) \tag{14}$$

Split $\Omega_{it}(\alpha_{it})$ into 2^s number of subregions. For 1-AMC ($s = 1$) the division is given by Eq. (15), and for 2-AMC it is given by Eq. (16).

$$\int_{a_d}^{b_d} \cdot\cdot \int_{a_k}^{b_k} \cdots \int_{a_1}^{b_1} f(x)dx = \int_{a_d}^{b_d} \cdot\cdot \int_{a_k}^{c} \cdots \int_{a_1}^{b_1} f(x)dx + \int_{a_d}^{b_d} \cdot\cdot \int_{c}^{b_k} \cdots \int_{a_1}^{b_1} f(x)dx \tag{15}$$

For 2-AMC ($s = 2$) the division is given by Eq. (24)

$$\begin{aligned}\int_{a_d}^{b_d} \cdots \int_{a_{k1}}^{b_{k1}} \cdots \int_{a_{k2}}^{b_{k2}} \cdots \int_{a_1}^{b_1} f(x)dx = &\int_{a_d}^{b_d} \cdots \int_{a_{k1}}^{c_1} \cdots \int_{a_{k2}}^{c_2} \cdots \int_{a_1}^{b_1} f(x)dx + \int_{a_d}^{b_d} \cdots \int_{c_1}^{b_{k1}} \cdots \int_{a_{k2}}^{c_2} \cdots \int_{a_1}^{b_1} f(x)dx \\ &+ \int_{a_d}^{b_d} \cdots \int_{a_{k1}}^{c_1} \cdots \int_{c_2}^{b_{k2}} \cdots \int_{a_1}^{b_1} f(x)dx + \int_{a_d}^{b_d} \cdots \int_{c_1}^{b_{k1}} \cdots \int_{c_2}^{b_{k2}} \cdots \int_{a_1}^{b_1} f(x)dx\end{aligned} \tag{16}$$

where, $c_m \in (a_{km}, b_{km})$, $1 \leq km \leq d$ for $m = 1, 2$. In each iteration it s distinct coordinates are divided. If promising region is divided into equal sub regions choose $c_m = (a_{km} - b_{km})/2$ for $m = 1, 2, \ldots, s$.

Step 5 Increase iteration number by $it = it + 1$.

Step 6 if $it < M$ go to step 2.

Step 7 The estimated integral is $\hat{I}_{it=M}$.

4. RESULTS AND DISCUSSION

The practical configuration is shown in Fig. 1, and parameters of the magnet are shown in Table 1. The objective of this paper is to calculate the force between the two ring magnets by proposed s-MC and validate the proposed technique by other methods and practical testing in the laboratory. The flowchart of s-MC is given in Fig. 8.

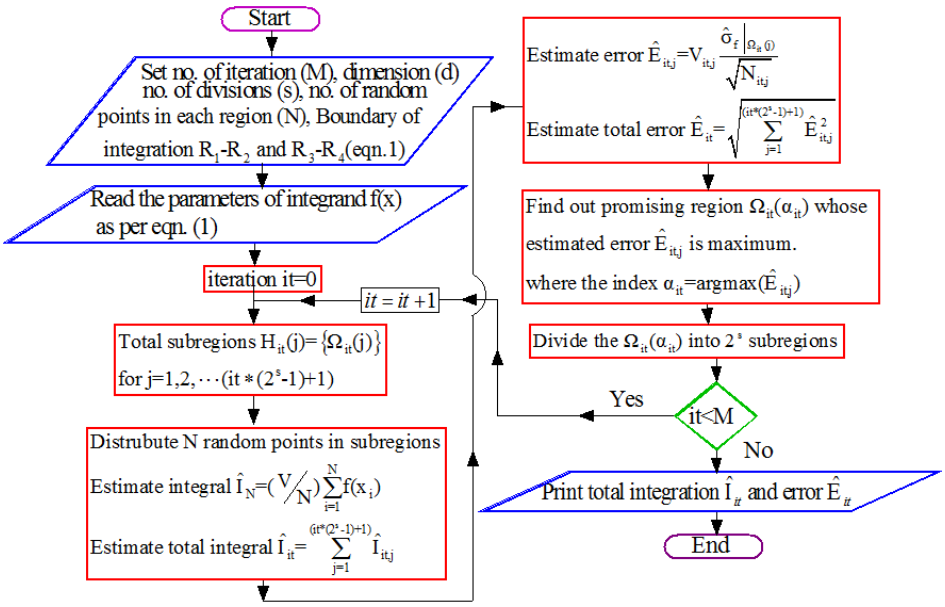

Figure 8. Flow chart for s-MC method.

4.1. Results of the Proposed Technique

Dimensions of the problem (1 and 2), $d = 4$, number of iteration $M = 50$ and number of random samples in each region $N = 25000$. A MATLAB code is developed to estimate the axial force on inner magnet. Let the inner magnet displaced by $x = 0$, $y = 0$ and $z = 0.002$ m. This is an axial displacement, so the axial force F_a will be calculated. Two detailed outputs are given, first 1-MC and then 2-MC. In Table 2, output from 1-MC is given, up to the third iteration.

In iteration 0, the estimated integral is actually the basic MC over the whole domain Ω. In iteration 1, Ω is divided into two (2^1) sub regions: $\Omega_1(1)$ and $\Omega_1(2)$. The basic MC is applied to each region and $\Omega_1(2)$ becomes the promising region due to high estimated error. So in iteration 2, $\Omega_1(2)$ is divided into another two sub-regions $\Omega_2(2)$ and $\Omega_2(2)$. In this way the iteration progresses and final estimated integral is given by the summation of basic MC integral of all sub-regions in the final Mth iteration. Table 3 represents the output from 2-MC. Here in iteration 1Ω is divided into four (2^2) sub-regions and the promising region is $\Omega_1(2)$, so it is divided into another four sub-regions, thus the total number of sub-regions in iteration 2 is seven and $\Omega_2(2)$ is the promising region. Fig. 9 represents the comparison of estimated error between 1-MC and 2-MC. It is clear that 2-MC algorithm has lower estimated error

Table 2. Output of 1-MC for rotor magnet displacement (0, 0, 0.002).

Iteration number it	Region collection H_{it}	Sub region $\Omega_{it}(j)$	Estimated Integral $\hat{I}_{it,j}$	Estimated total Integral $\hat{I}_{it}$	Estimated Error $\hat{E}_{it,j}$	Estimated total error $\hat{E}_{it}$
0	H_0	$\Omega_0(1)$	173.153	**173.151**	0.251	**0.251**
1	H_1	$\Omega_1(1)$	58.151	**172.364**	0.063	**0.155**
		$\Omega_1(2)$	114.213		**0.142**	
2	H_2	$\Omega_2(1)$	58.11	**171.251**	0.063	**0.115**
		$\Omega_2(2)$	72.432		**0.081**	
		$\Omega_2(3)$	40.668		0.051	

Table 3. Output of 2-MC for inner magnet displacement (0, 0, 0.002).

Iteration number it	Region collection H_{it}	Sub region $\Omega_{it}(j)$	Estimated Integral $\hat{I}_{it,j}$	Estimated total Integral $\hat{I}_{it}$	Estimated Error $\hat{E}_{it,j}$	Estimated total error $\hat{E}_{it}$
0	H_0	$\Omega_0(1)$	173.113	**173.113**	**0.242**	**0.242**
1	H_1	$\Omega_1(1)$	31.210	**172.321**	0.041	**0.153**
		$\Omega_1(2)$	56.341		0.087	
		$\Omega_1(3)$	59.230		**0.107**	
		$\Omega_1(4)$	25.540		0.052	
2	H_2	$\Omega_2(1)$	31.210	**170.153**	0.041	**0.109**
		$\Omega_2(2)$	56.341		**0.087**	
		$\Omega_2(3)$	13.710		0.005	
		$\Omega_2(4)$	17.301		0.003	
		$\Omega_2(5)$	15.010		0.001	
		$\Omega_2(6)$	11.041		0.002	
		$\Omega_2(7)$	25.540		0.052	

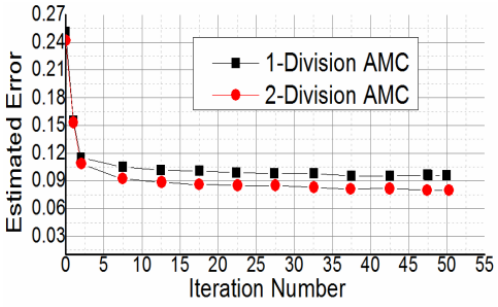

Figure 9. Estimated errors in 1-AMC and 2-AMC algorithm during 50 iterations.

than 1-MC. In the similar manner force on inner magnet for different displacement is calculated and plotted in Fig. 10.

4.2. Results of FEM Analysis

Figure 3 shows the magneto static analysis with flux distribution for nominal position, axially and radially shifted positions of inner magnet in X-Z plane, respectively. It is observed that in nominal position the resultant force on the inner magnet is zero. If it is shifted upwards as shown in Fig. 3(b),

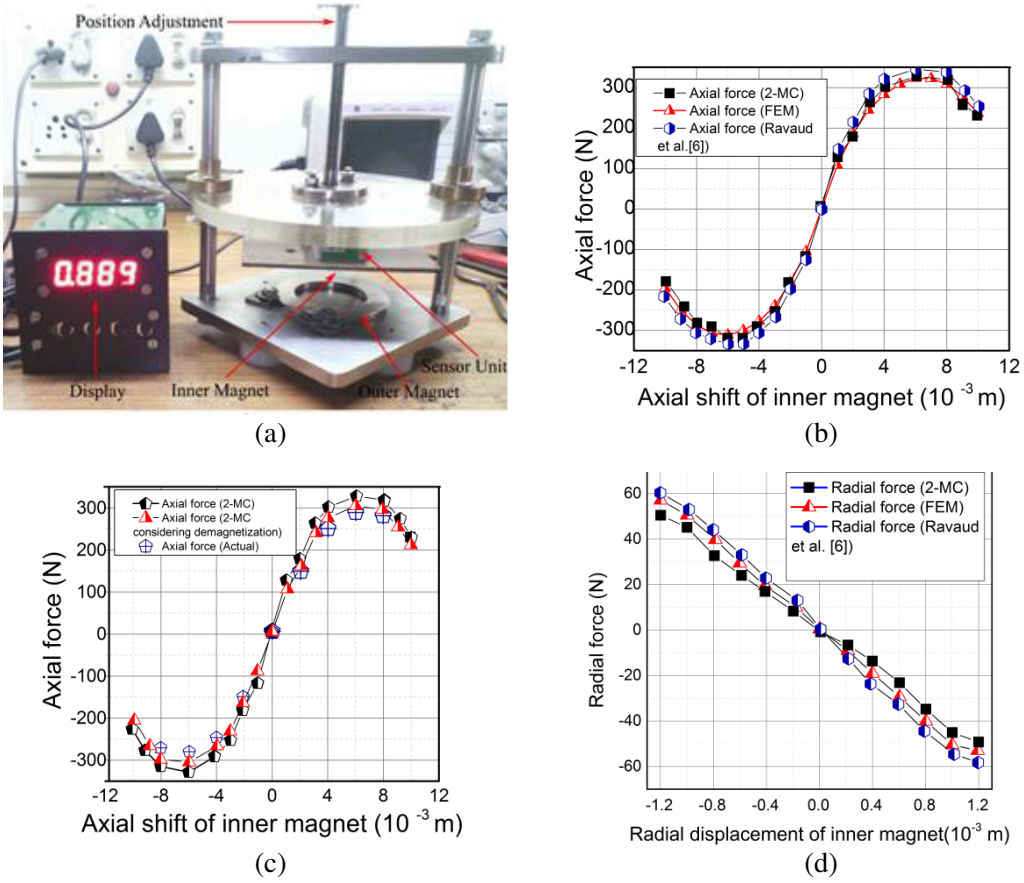

Figure 10. (a) Test set-up to measure force between two ring magnets. (b) Comparison of axial force computed by FEM, 2-MC and Ref. (Ravaud et al., 2009). (c) Closeness of 2-MC considering demagnetization with experimental results. (d) Comparison of radial force computed by FEM, 2-MC and Ref. (Ravaud et al., 2009).

a destabilizing resultant force acts upwards on the inner magnet. If the inner magnet shifted in radial direction as shown in Fig. 3(c), a stabilizing resultant force acts on it. The force on inner magnet at different axial position is calculated using FEM and plotted in Fig. 10. If the derivative of force with respect to displacement is calculated from Figs. 10(b) and 10(d), it is observed that derivative of axial force is positive, and for radial force derivative is negative. It signifies that the axial force is destabilizing and radial force is stabilizing in nature.

4.3. Results of Laboratory Testing

A laboratory test setup is fabricated to measure the axial force between two ring magnets, as shown in Fig. 10(a). There is an arrangement to hold the two ring magnets. By a screw and nut arrangement inner magnet can be placed at different axial positions, whereas the outer magnet is fixed. A sensor unit is used to measure the axial repulsive force between the stator and rotor magnets, and a display is used to show the calibrated results. The force on rotor magnet at different axial position is obtained from the testing and plotted in Fig. 10(c).

5. VALIDATION OF THE PROPOSED TECHNIQUE

A comparison of axial force (Fig. 10(b)) and radial force (Fig. 10(d)) is represented using s-MC, FEM & Ravaud et al. [6] respectively. It is observed that results from these three methods are in close

Table 4. Computation time for magnetic force calculation.

Quadrature method of integration	Finite element method (FEM)	Adaptive Monte Carlo Method (AMC)	Proposed 2-MC method Upto 20 iterations
160 sec	28 sec	16 sec	11 sec

agreement with each other. Fig. 10(c) represents the validation of 2-MC by experimental result. It is observed that if the self-demagnetization is considered, 2-MC gives excellent results with respect to practical test results. A comparison has been carried out to observe the computation time for calculating the magnetic force by different methods (Table 4). Maximum time is taken by quadrature method of integration which is natural as at higher dimension quadrature method becomes very complex. FEM takes moderate execution time of 28 sec more than 2-MC because 2-MC does not calculate for all the discrete magnetic surfaces with equal importance. It splits only the promising region with high estimated error. Whereas FEM consider all the discrete magnetic surfaces on inner and outer magnet pole faces. The proposed method also executes in lesser time than AMC method because AMC optimally selects the sample density at each iterations whereas s-MC considers the constant sample density thus avoiding some calculations. Thus s-MC reduces the computation burden also.

6. CONCLUSION

The objective is to calculate the force between stator and rotor magnets of a radial passive bearing. Existing analytical or semi-analytical methods have lower accuracy, whereas FEM has high accuracy but also high computational time. This paper proposes a 3D numerical method where the multidimensional integration is solved using Monte Carlo technique with general division approach (s-MC). The proposed technique minimizes the complexity of the problem as well as reducing the computational time compared to other methods. In most of the cases, the expression of magnetic force contains complicated implicit or elliptic function. The great advantage of the proposed method is that it does not depend on the type of the integrand. Integrand may have an implicit or elliptical function, and it does not matter for the proposed technique. The multidimensional integration is numerically solved by both 1-MC and 2-MC methods using MATLAB. It is observed that the 2-AMC method gives better result, and its estimated standard error is also less. In support of the proposed technique, FEM semi-analytical analysis has been carried out. Finally, the test result is obtained from the laboratory, and it is observed that laboratory result is also in close agreement with the results from the proposed technique. The computation time of the proposed method is less than the existing methods: quadrature, FEM and AMC.

ACKNOWLEDGMENT

This research work is sponsored by the Science and Engineering Research Board (SERB), New Delhi, India, order No. SR/S3/EECE/0164/2012.

REFERENCES

1. Yonnet, J. P., "Passive magnetic bearings with permanent magnets," *IEEE Trans. Magn.*, Vol. 14, No. 5, 803–805, 1978.
2. Fang, J., Y. Le, J. Sun, and K. Wang, "Analysis and design of passive magnetic bearing and damping system for high-speed compressor," *IEEE Trans. Magn.*, Vol. 48, No. 6, 2528–2537, 2012.
3. Wang, F., J. Wang, Z. Kong, and F. Zhang, "Radial and axial force calculation of BLDC motor with passive magnetic bearing," *4th International Power Electronics and Motion Control Conference, IPEMC 2004*, Vol. 1, 290–293, Xi'an, China, Aug. 14–16, 2004.
4. Mukhopadhyay, S. C., T. Ohji, M. Iwahara, and A. Member, "Modeling and control of a new horizontal-shaft hybrid-type magnetic bearing," *IEEE Trans. Ind. Electron.*, Vol. 47, No. 1, 100–108, 2000.

5. Tan, Q., W. Li, and B. Liu, "Investigations on a permanent magnetic hydrodynamic hybrid journal bearing," *Tribol. Int.*, Vol. 35, No. 7, 443–448, 2002.
6. Ravaud, R., G. Lemarquand, and V. Lemarquand, "Force and stiffness of passive magnetic bearings using permanent magnets. Part 1: Axial magnetization," *IEEE Trans. Magn.*, Vol. 45, No. 7, 2996–3002, 2009.
7. Bekinal, S. I., A. R. Tumkur Ramakrishna, and S. Jana, "Analysis of axially magnetized permanent magnetic bearing characteristics," *Progress In Electromagnetics Research B*, Vol. 44, 327–343, 2012.
8. Paden, B., N. Groom, and J. F. Antaki, "Design formulas for permanent-magnet bearings," *ASME J. Mech. Des.*, Vol. 125, No. 3, 734–738, 2003.
9. Ravaud, R., G. Lemarquand, V. Lemarquand, and C. Depollier, "Discussion about the analytical calculation of the magnetic field created by permanent magnets," *Progress In Electromagnetics Research B*, Vol. 11, 281–297, 2009.
10. Lijesh, K. P. and H. Hirani, "Development of analytical equations for design and optimization of axially polarized radial passive magnetic bearing," *Journal of Tribology*, Vol. 137, 011103–9, 2015.
11. Santra, T., D. Roy, and S. Yamada, "Calculation of force between two ring magnets using adaptive Monte Carlo technique with experimental verification," *Progress In Electromagnetics Research M*, Vol. 49, 181–193, 2016.
12. Pennanen, T. and M. Koivu, "An adaptive importance sampling technique," *Monte Carlo and Quasi-Monte Carlo Methods*, 443–455, Springer, 2004.
13. Rakotoarison, H. L., J. P. Yonnet, and B. Delinchant, "Using coulombian approach for modelling scalar potential and magnetic field of a permanent magnet with radial polarization," *IEEE Trans. Magn.*, Vol. 43, No. 4, 1261–1264, 2007.
14. Wangsness, R. K., *Electromagnetic Fields*, Wiley, New York, 1979.
15. Parker, R. J., "Analytical methods for permanent magnet design," *Electro-Technology*, 1960.
16. Mishra, M. and N. Gupta, "Monte Carlo integration technique for the analysis of electromagnetic Scattering from conducting surfaces," *Progress In Electromagnetics Research*, Vol. 79, 91–106, 2008.
17. Alrefaei, M. H. and H. M. Abdul-Rahman, "An adaptive Monte Carlo integration algorithm with general division approach," *Math. Comput. Simul.*, 2007, doi:10.1016/j.matcom.2007.09.009.